

# Detecting OOD Samples via Optimal Transport Scoring Function

Heng Gao  
ISTBI

Fudan University  
Shanghai, China  
hgao22@m.fudan.edu.cn

Zhuolin He  
School of Computer Science

Fudan University  
Shanghai, China  
zlhe22@m.fudan.edu.cn

Jian Pu\*

ISTBI  
Fudan University  
Shanghai, China  
jianpu@fudan.edu.cn

**Abstract**—To deploy machine learning models in the real world, researchers have proposed many OOD detection algorithms to help models identify unknown samples during the inference phase and prevent them from making untrustworthy predictions. Unlike methods that rely on extra data for outlier exposure training, post hoc methods detect Out-of-Distribution (OOD) samples by developing scoring functions, which are model agnostic and do not require additional training. However, previous post hoc methods may fail to capture the geometric cues embedded in network representations. Thus, in this study, we propose a novel score function based on the optimal transport theory, named OTOD, for OOD detection. We utilize information from features, logits, and the softmax probability space to calculate the OOD score for each test sample. Our experiments show that combining this information can boost the performance of OTOD with a certain margin. Experiments on the CIFAR-10 and CIFAR-100 benchmarks demonstrate the superior performance of our method. Notably, OTOD outperforms the state-of-the-art method GEN by 7.19% in the mean FPR@95 on the CIFAR-10 benchmark using ResNet-18 as the backbone, and by 12.51% in the mean FPR@95 using WideResNet-28 as the backbone. In addition, we provide theoretical guarantees for OTOD. The code is available in <https://github.com/HengGao12/OTOD>.

**Index Terms**—Out-of-distribution detection, Wasserstein distances, Deep neural networks, Machine learning safety

## I. INTRODUCTION

To prevent machine learning models from producing untrustworthy predictions and being overconfident on Out-of-Distribution (OOD) inputs [1], various OOD detection algorithms have been proposed to enable models to distinguish whether a test sample comes from in-distribution (ID) data or unseen domains.

The post hoc-based methods identify OOD samples by developing scoring functions, which are free of training and model agnostic. In MSP [2], Hendrycks et al. first propose a strong baseline that utilizes the statistics of softmax probability outputs to identify outliers. ODIN [10] proposes detecting OOD samples by adding input perturbation and temperature scaling. In EBO [3], the authors develop an energy-based score function that uses information from the model’s logits outputs, surpassing many softmax-based scores and generative-based methods. In recent work, GEN [4] proposes using generalized entropy to calculate the OOD scores of test samples. However,

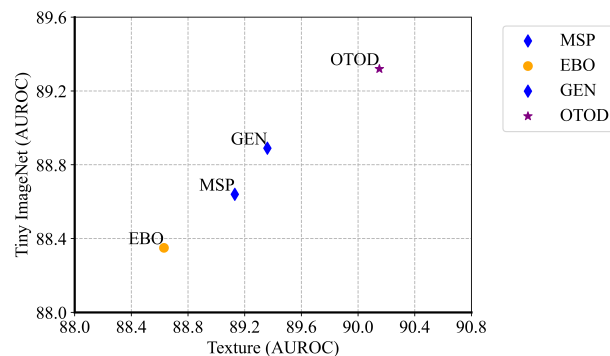


Fig. 1. The AUROC (in percentage) of four OOD detection methods using ResNet-18 [5] trained on CIFAR-10 [6]. The OOD datasets are Tiny ImageNet (TIN) [11] and Texture [14]. Methods marked with blue  $\diamond$  use the softmax probability input; methods marked with orange  $\circ$  use the logits inputs. Our proposed method OTOD (marked with purple  $\star$ ) uses information from logits, softmax probability, and features.

limited attention is paid to study how to develop a score function based on optimal transport distances, which possess good theoretical properties [7] and are capable of capturing the spatial discrepancies between probability distributions [23].

Therefore, in this paper, we develop a post hoc method that leverages the optimal transport distance [7], also known as Wasserstein distance, to calculate OOD scores without any training techniques or modifying the network architecture. Specifically, we first employ Wasserstein-1 distance to calculate OOD scores using features extracted from the penultimate layer of the pre-trained neural network. Unlike methods that utilize statistical distances, such as MDS [8] and KLM [9], OTOD does not require estimating the empirical class mean and covariance for the ID data during the OOD testing phase. Then, we combine information from the logits and the softmax probability space to calculate OOD scores. We find that integrating this information helps to improve the OOD detection results. Moreover, we apply the temperature scaling technique [10] to further enhance the OOD detection performance. The experiments on the CIFAR-10 and CIFAR-100 [6] benchmarks demonstrate the superior performance of OTOD, which outperforms many state-of-the-art post hoc methods. Furthermore, we provide theoretical guarantees for

\*Corresponding author.

OTOD.

The main contributions of our paper are: (1) We develop a novel post hoc method based on optimal transport theory, named OTOD, to calculate OOD scores of test samples without using any in-distribution data. (2) We find that the combination of features, logits, and softmax probability inputs allows OTOD to achieve non-trivial improvements in several commonly used metrics (the FPR@95 and AUROC) on the CIFAR-10/100 [6] benchmarks. (3) Both empirical and theoretical results demonstrate the superior performance of OTOD.

## II. BACKGROUND

### A. Wasserstein Distances

Now we introduce the definition of Wasserstein distances.

**Definition 1** (Wasserstein distances [7]). *Denote  $(\mathbf{X}, d)$  as a Polish metric space and let  $p \in [1, \infty)$ . For any two probability measures  $\mu, \nu$  on  $\mathbf{X}$ , the Wasserstein distance of order  $p$  between  $\mu$  and  $\nu$  is defined as follows:*

$$\mathcal{W}_p(\mu, \nu) = \left( \inf_{\pi \in \Pi(\mu, \nu)} \int_{\mathbf{X}} d(x, y)^p d\pi(x, y) \right)^{1/p},$$

where  $\Pi(\mu, \nu)$  is the set of all joint probability measures on  $\mathbf{X} \times \mathbf{X}$  whose marginals are  $\mu$  and  $\nu$ .

Particularly, let  $p = 1$ , we can obtain the  $\mathcal{W}_1$  distance, also known as Kantorovich–Rubinstein distance, which can be written in the following form,

$$\mathcal{W}_1(\mu, \nu) = \sup_{\|\psi\|_{\text{L}} \leq 1} \left\{ \int_{\mathbf{X}} \psi d\mu - \int_{\mathbf{X}} \psi d\nu \right\},$$

where  $\psi \in L^1(\mu)$  is c-convex and 1-Lipschitz,  $\|\cdot\|_{\text{L}}$  denotes the Lipschitz norm of function  $\psi$ .

### III. OPTIMAL TRANSPORT SCORING FUNCTION

The main idea of our method is to develop a score function based on Optimal Transport theory [7] to calculate the OOD scores for test samples. Our method consists of two parts: (i) Wasserstein-1 score calculation (in Section III-A); (ii) multi-scale information integration (in Section III-B). We also provide theoretical guarantees for OTOD partially (in Section III-C).

#### A. Optimal Transport Score Calculation

For each input image  $\mathbf{x} \in \mathbf{X}$ ,  $\mathbf{X}$  is the input space, the feature of the given sample is denoted by  $\mathbf{f} \in \mathbb{R}^d$ . Then, we normalize feature  $\mathbf{f}$  by using  $L^2$  normalization. Denote the normalized feature as  $\hat{\mathbf{f}} = \mathbf{f}/\|\mathbf{f}\|_2$ . In this case,  $\hat{\mathbf{f}}$  can be approximated as a d-dimensional distribution.

Afterwards, we use  $\mathcal{W}_1$  distance to calculate the OOD score for each test sample. To be specific, the Wasserstein-1 OOD score for sample  $\mathbf{x}$  takes the form as

$$\hat{S}_{\mathcal{W}_1}(\hat{\mathbf{f}}) = -\min \left[ \mathcal{W}_1(\hat{\mathbf{f}}, \mathbf{u}), \mathcal{W}_1(\hat{\mathbf{f}}, \mathbf{o}) \right], \quad (1)$$

where  $\mathbf{u}$  is a mean vector,  $\mathbf{o}$  is a zero vector. Note that, here we have a model ensemble effect by using both the mean vector and the zero vector to calculate the Wasserstein-1 score.

#### B. Multi-scale Information Integration

To enhance the performance of OTOD, we further integrate the information contained in logits and softmax probability. Specifically, denote the logits of the given image sample as  $\mathbf{l} \in \mathbb{R}^K$ ,  $K$  is the number of classes. Denote the softmax probability as  $\mathbf{p} \in [0, 1]^K$ . Then, we also normalize vector  $\mathbf{l}$ ,  $\mathbf{p}$  and perform the same calculation as equation (1). Likewise, we denote the normalized logits and softmax probability as  $\hat{\mathbf{l}}, \hat{\mathbf{p}}$ . Therefore, the whole Wasserstein-1 score can be written as

$$\tilde{S}_{\mathcal{W}_1}(\hat{\mathbf{f}}, \hat{\mathbf{l}}, \hat{\mathbf{p}}) = \alpha_1 \hat{S}_{\mathcal{W}_1}(\hat{\mathbf{f}}) + \alpha_2 \hat{S}_{\mathcal{W}_1}(\hat{\mathbf{l}}) + \alpha_3 \hat{S}_{\mathcal{W}_1}(\hat{\mathbf{p}}), \quad (2)$$

where

$$\sum_{i=1}^3 \alpha_i = 1, \alpha_i \in [0, 1]. \quad (3)$$

Moreover, we adapt the temperature scaling technique from ODIN [10] to OTOD to further enlarge the discrepancy between ID and OOD softmax probability. Hence, the final score takes the form of the following:

$$S_{\mathcal{W}_1}(\hat{\mathbf{f}}, \hat{\mathbf{l}}, \tilde{\mathbf{p}}) = \alpha_1 \hat{S}_{\mathcal{W}_1}(\hat{\mathbf{f}}) + \alpha_2 \hat{S}_{\mathcal{W}_1}(\hat{\mathbf{l}}) + \alpha_3 \hat{S}_{\mathcal{W}_1}(\tilde{\mathbf{p}}), \quad (4)$$

where  $\alpha_1, \alpha_2, \alpha_3$  satisfy equation (3),  $\tilde{\mathbf{p}}$  is the normalization of  $\text{Softmax}(1/T)$ ,  $T$  is the temperature.

#### C. Theoretical Guarantee

In this section, we provide the theoretical guarantee for the feature part of OTOD (the Equation (1)) approximately.

To this end, we assume that a class conditional distribution in the model’s penultimate layer’s feature space follows the multivariate Gaussian distribution [20], which is empirically demonstrated in [8]. Herein, we also verify this fact in Fig. 2 (a). In addition, after the normalization operation, the feature distribution does not change markedly (see Fig. 2(b)). Therefore, we can still use the multivariate Gaussian assumption [20], i.e.,  $\hat{\mathbf{f}}|y_i \sim \mathcal{N}(\boldsymbol{\mu}_i, \Sigma)$ , where  $\boldsymbol{\mu}_i$  is the mean of class  $y_i, i = 1, \dots, K$ ,  $\Sigma$  is the covariance matrix.

Then, we define the Mean Discrepancy (MD) metric of a given score function, which is a concept borrowed from Maximum Mean Discrepancy (MMD) [21] that quantifies how well OTOD discerns ID samples from the OOD ones. The definition can be stated as follows:

**Definition 2** (Mean Discrepancy). *Denote  $S : \tilde{X} \rightarrow \mathbb{R}$  as a score function, where  $\tilde{X}$  is the model’s penultimate layer’s feature space. Then, let  $P_{\tilde{X}}^{\text{in}}$  be the in-distribution marginal probability distribution on  $\tilde{X}$ ,  $P_{\tilde{X}}^{\text{ood}}$  be the OOD distribution. Therefore, the Mean Discrepancy (MD) for score function  $S$  can be written as*

$$\mathbb{E}_{\mathbf{x} \sim P_{\tilde{X}}^{\text{in}}} [S(\mathbf{x})] - \mathbb{E}_{\mathbf{x} \sim P_{\tilde{X}}^{\text{ood}}} [S(\mathbf{x})].$$

Assume that the out-of-distribution data distribution  $P_{\tilde{X}}^{\text{ood}} = \mathcal{N}(\boldsymbol{\mu}^{\text{ood}}, \Sigma)$  [20], herein  $\boldsymbol{\mu}^{\text{ood}}$  is the mean of OOD data. Then, we can show the following Theorem, which gives the upper bound of Equation (1)’s MD.

TABLE I  
EVALUATION ON THE CIFAR-10 [3] BENCHMARK USING RESNET-18 [5] AND WIDERESNET-28 [16] AS THE BACKBONE.

| Model         | Methods            | CIFAR-100    |              | TIN          |              | MNIST        |              | OOD Datasets SVHN |              | Texture      |              | Place365     |              | Average      |              | ID ACC       |
|---------------|--------------------|--------------|--------------|--------------|--------------|--------------|--------------|-------------------|--------------|--------------|--------------|--------------|--------------|--------------|--------------|--------------|
|               |                    | FPR@95 ↓     | AUROC ↑      | FPR@95 ↓     | AUROC ↑      | FPR@95 ↓     | AUROC ↑      | FPR@95 ↓          | AUROC ↑      | FPR@95 ↓     | AUROC ↑      | FPR@95 ↓     | AUROC ↑      | FPR@95 ↓     | AUROC ↑      |              |
| ResNet-18 [5] | MSP [2]            | 59.82        | 86.73        | 47.33        | 88.64        | 19.22        | 93.95        | <b>23.82</b>      | 91.68        | 40.20        | 89.13        | 41.67        | 89.35        | 38.68        | 89.91        | 95.22        |
|               | ODIN [10]          | 84.87        | 79.55        | 84.59        | 81.18        | <b>15.39</b> | <b>96.60</b> | 69.04             | 84.62        | 83.19        | 83.86        | 76.62        | 83.87        | 68.95        | 84.95        | 95.22        |
|               | MDS [8]            | 95.83        | 49.85        | 94.68        | 49.60        | 65.67        | 66.86        | 44.56             | 84.38        | 98.37        | 47.82        | 91.02        | 62.76        | 81.69        | 60.21        | 95.22        |
|               | EBO [3]            | 72.69        | 85.55        | 63.68        | 88.35        | 15.49        | 96.32        | 29.34             | <b>92.60</b> | 60.43        | 88.63        | 56.38        | 89.63        | 49.67        | 90.18        | 95.22        |
|               | Gram [19]          | 95.83        | 49.85        | 94.68        | 49.60        | 65.67        | 66.86        | 44.56             | 84.38        | 98.37        | 47.82        | 91.02        | 62.76        | 81.69        | 60.21        | 95.22        |
|               | KLM [9]            | 92.23        | 77.48        | 81.97        | 80.02        | 68.80        | 87.31        | 69.12             | 83.54        | 70.66        | 82.21        | 96.72        | 78.14        | 79.92        | 81.45        | 95.22        |
|               | GEN [4]            | 63.63        | 86.71        | 52.09        | 88.89        | 18.01        | 95.00        | 24.08             | 92.18        | 46.12        | 89.36        | 46.12        | <b>89.74</b> | 41.68        | 90.31        | 95.22        |
|               | OTOD (Ours)        | <b>45.19</b> | <b>87.75</b> | <b>40.01</b> | <b>89.32</b> | 23.64        | 93.97        | 24.34             | 92.35        | <b>33.41</b> | <b>90.15</b> | <b>40.36</b> | 88.83        | <b>34.49</b> | <b>90.40</b> | <b>95.22</b> |
|               | WideResNet-28 [16] | MSP [2]      | 51.90        | 88.56        | 41.00        | 90.34        | 16.07        | 95.01             | 17.59        | 93.85        | 51.87        | 89.01        | 47.56        | 89.53        | 37.67        | 91.05        |
| ODIN [10]     |                    | 84.12        | 80.55        | 81.61        | 82.34        | 17.77        | 95.91        | 79.61             | <b>80.08</b> | 90.88        | 81.39        | 82.61        | 82.59        | 72.77        | 83.81        | 95.81        |
| MDS [8]       |                    | 53.99        | 85.93        | 44.63        | 88.09        | 37.77        | <b>87.47</b> | <b>9.60</b>       | <b>97.71</b> | <b>12.10</b> | <b>97.71</b> | 49.28        | 86.77        | 34.56        | 90.62        | 95.76        |
| EBO [3]       |                    | 65.27        | 88.10        | 53.56        | 90.55        | <b>11.58</b> | <b>97.38</b> | 18.61             | 94.98        | 70.03        | 88.28        | 60.78        | 89.85        | 46.64        | 91.52        | 95.81        |
| Gram [19]     |                    | 81.97        | 67.56        | 69.63        | 76.80        | 51.00        | 81.07        | 24.22             | 95.26        | 94.64        | 73.89        | 75.09        | 74.31        | 66.09        | 78.15        | 95.81        |
| KLM [9]       |                    | 80.71        | 79.32        | 82.76        | 81.28        | 74.03        | 87.59        | 67.28             | 86.82        | 88.42        | 82.08        | 80.38        | 79.66        | 78.93        | 82.79        | 95.81        |
| GEN [4]       |                    | 61.88        | 88.44        | 50.94        | 90.71        | 12.73        | 97.06        | 17.88             | 94.95        | 65.86        | 88.76        | 57.34        | 89.98        | 44.44        | <b>91.65</b> | 95.81        |
| OTOD (Ours)   |                    | <b>40.46</b> | <b>89.52</b> | <b>33.56</b> | <b>90.98</b> | 22.47        | 94.14        | 19.37             | 94.38        | 37.72        | 90.04        | <b>38.00</b> | <b>90.14</b> | <b>31.93</b> | 91.53        | <b>95.81</b> |

TABLE II  
EVALUATION ON THE CIFAR-100 [3] BENCHMARK USING RESNET-18 [5] AND WIDERESNET-28 [16] AS THE BACKBONE.

| Model         | Methods            | CIFAR-100    |              | TIN          |              | MNIST        |              | OOD Datasets SVHN |              | Texture      |              | Place365     |              | Average      |              | ID ACC       |
|---------------|--------------------|--------------|--------------|--------------|--------------|--------------|--------------|-------------------|--------------|--------------|--------------|--------------|--------------|--------------|--------------|--------------|
|               |                    | FPR@95 ↓     | AUROC ↑      | FPR@95 ↓     | AUROC ↑      | FPR@95 ↓     | AUROC ↑      | FPR@95 ↓          | AUROC ↑      | FPR@95 ↓     | AUROC ↑      | FPR@95 ↓     | AUROC ↑      | FPR@95 ↓     | AUROC ↑      |              |
| ResNet-18 [5] | MSP [2]            | 59.12        | 78.54        | 49.98        | 82.22        | 63.47        | 73.54        | 55.44             | 79.37        | 61.24        | 78.07        | 55.40        | 79.61        | 57.44        | 78.56        | 77.17        |
|               | ODIN [10]          | 60.98        | 78.03        | 55.86        | 81.53        | 50.36        | 82.09        | 62.16             | 75.56        | 59.83        | <b>80.46</b> | 58.51        | 79.80        | 57.95        | 79.58        | 77.17        |
|               | MDS [8]            | 89.97        | 52.50        | 81.37        | 58.72        | 72.16        | 63.88        | 71.10             | 67.55        | 76.00        | 73.38        | 83.97        | 58.60        | 79.10        | 62.44        | <b>77.33</b> |
|               | EBO [3]            | 58.88        | 79.01        | 52.53        | 82.51        | 57.57        | 77.30        | 50.84             | 82.67        | 60.21        | 79.33        | 56.47        | 79.81        | 56.08        | <b>80.11</b> | 77.17        |
|               | Gram [19]          | 91.74        | 50.38        | 91.96        | 51.16        | <b>45.17</b> | <b>85.82</b> | <b>22.50</b>      | <b>95.22</b> | 90.30        | 69.27        | 93.69        | 45.01        | 72.56        | 66.14        | 77.17        |
|               | KLM [9]            | 88.62        | 74.18        | 70.62        | 79.57        | 63.70        | 71.94        | 58.02             | 80.07        | 75.50        | 76.32        | 83.52        | 76.04        | 73.33        | 76.35        | 77.17        |
|               | GEN [4]            | <b>58.56</b> | <b>79.39</b> | <b>49.44</b> | <b>83.28</b> | 61.42        | 75.66        | 53.68             | 81.53        | 60.78        | 79.53        | <b>55.03</b> | <b>80.57</b> | 56.49        | 79.99        | 77.17        |
|               | OTOD (Ours)        | 59.38        | 78.91        | 50.39        | 83.04        | 56.96        | 76.75        | 50.47             | 81.99        | <b>58.38</b> | 79.36        | 55.24        | 80.08        | <b>55.14</b> | 80.02        | 77.17        |
|               | WideResNet-28 [16] | MSP [2]      | <b>55.70</b> | 80.45        | 49.58        | 83.01        | 50.50        | 79.61             | 54.58        | 81.61        | 66.18        | 75.86        | 57.49        | 79.69        | 55.67        | 80.04        |
| ODIN [10]     |                    | 59.11        | 79.62        | 57.56        | 81.31        | 47.28        | <b>83.15</b> | 72.03             | 72.57        | 66.23        | 77.88        | 64.07        | 79.24        | 61.05        | 78.96        | 80.07        |
| MDS [8]       |                    | 74.32        | 75.04        | 55.47        | 81.83        | 71.04        | 70.24        | 34.13             | 90.85        | <b>38.97</b> | 91.07        | 65.11        | 78.46        | 56.51        | 81.25        | <b>80.33</b> |
| EBO [3]       |                    | 57.16        | 81.33        | 51.16        | 83.80        | <b>44.73</b> | 84.08        | 53.44             | 83.39        | 66.97        | 76.46        | 60.92        | 79.70        | 55.73        | <b>81.46</b> | 80.07        |
| Gram [19]     |                    | 87.34        | 64.90        | 66.87        | 75.43        | 56.29        | 80.55        | <b>21.70</b>      | <b>93.95</b> | 76.40        | 80.25        | 83.60        | 64.05        | 65.37        | 76.52        | 80.07        |
| KLM [9]       |                    | 74.16        | 75.76        | 73.19        | 79.61        | 66.40        | 74.41        | 59.34             | 79.82        | 83.12        | <b>72.78</b> | 81.53        | 75.51        | 72.96        | 76.32        | 80.07        |
| GEN [4]       |                    | 55.82        | 81.33        | 48.73        | 84.29        | 48.78        | 80.45        | 53.16             | 83.40        | 65.98        | 76.97        | <b>57.32</b> | <b>80.78</b> | <b>54.97</b> | 81.20        | 80.07        |
| OTOD (Ours)   |                    | 56.67        | <b>81.52</b> | <b>48.88</b> | <b>84.49</b> | 47.21        | 81.43        | 52.99             | 83.06        | 69.52        | 75.68        | 57.70        | 80.47        | 55.50        | 81.11        | 80.07        |

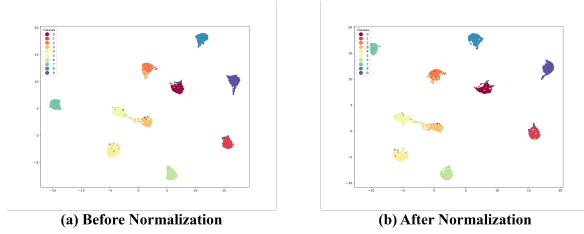


Fig. 2. UMAP [22] visualization of unnormalized (a) and normalized (b) feature distribution using WideResNet-28 [16] on the CIFAR-10 [3] benchmark.

**Theorem 1** (Mean Discrepancy Upper Bound). *Suppose that the diameter of  $\tilde{X}$  is bounded by  $D$ ,  $V(\tilde{X})$  is the volume of  $\tilde{X}$ . Consider the case where  $\tilde{X}$  is the normalized feature space. Then,  $\forall 1 \leq i \leq K$ , given the setups above, we have the following inequality:*

$$\mathbb{E}_{\hat{\mathbf{f}} \sim P_{\tilde{X}}^{in}} [\hat{S}_{W_1}(\hat{\mathbf{f}})] - \mathbb{E}_{\hat{\mathbf{f}} \sim P_{\tilde{X}}^{ood}} [\hat{S}_{W_1}(\hat{\mathbf{f}})] \leq 2\tilde{C}DV(\tilde{X})\|\mu_i - \mu^{ood}\|_{TV}, \quad (5)$$

where  $\|\cdot\|_{TV}$  represents the total variation norm,  $\tilde{C}$  is a constant.

*Proof.* Denote  $MD = \mathbb{E}_{\hat{\mathbf{f}} \sim P_{\tilde{X}}^{in}} [\hat{S}_{W_1}(\hat{\mathbf{f}})] - \mathbb{E}_{\hat{\mathbf{f}} \sim P_{\tilde{X}}^{ood}} [\hat{S}_{W_1}(\hat{\mathbf{f}})]$ , and the probability density function of  $P_{\tilde{X}}^{in}(\hat{\mathbf{f}})$  and  $P_{\tilde{X}}^{ood}(\hat{\mathbf{f}})$  as  $p_{\tilde{X}}^{in}(\hat{\mathbf{f}})$ ,  $p_{\tilde{X}}^{ood}(\hat{\mathbf{f}})$ , respectively. Then we have

$$MD \leq |\mathbb{E}_{\hat{\mathbf{f}} \sim P_{\tilde{X}}^{in}} [\hat{S}_{W_1}(\hat{\mathbf{f}})] - \mathbb{E}_{\hat{\mathbf{f}} \sim P_{\tilde{X}}^{ood}} [\hat{S}_{W_1}(\hat{\mathbf{f}})]|$$

$$\begin{aligned} &\leq \int_{\tilde{X}} W_1(\hat{\mathbf{f}}, \mathbf{u}) p_{\tilde{X}}^{in}(\hat{\mathbf{f}}) d\hat{\mathbf{f}} + \int_{\tilde{X}} W_1(\hat{\mathbf{f}}, \mathbf{u}) p_{\tilde{X}}^{ood}(\hat{\mathbf{f}}) d\hat{\mathbf{f}} \\ &\leq D \left[ \int_{\tilde{X}} \|\hat{\mathbf{f}} - \mathbf{u}\|_{TV} \cdot p_{\tilde{X}}^{in}(\hat{\mathbf{f}}) d\hat{\mathbf{f}} \right. \\ &\quad \left. + \int_{\tilde{X}} \|\hat{\mathbf{f}} - \mathbf{u}\|_{TV} \cdot p_{\tilde{X}}^{ood}(\hat{\mathbf{f}}) d\hat{\mathbf{f}} \right] \\ &\leq 2D \int_{\tilde{X}} \|\hat{\mathbf{f}} - \mathbf{u}\|_{TV} d\hat{\mathbf{f}} \\ &= 2DV(\tilde{X})\|\hat{\mathbf{f}}^* - \mathbf{u}\|_{TV} \\ &\leq 2\tilde{C}DV(\tilde{X})\|\mu_i - \mu^{ood}\|_{TV}, \end{aligned}$$

where  $\hat{\mathbf{f}}^* \in \tilde{X}$ ,  $\tilde{C}$  is a constant.  $\square$

Notice that, as  $\|\mu_i - \mu^{ood}\|_{TV} \rightarrow 0$ , the right-hand side of the inequality (5) approaches to 0, which implies that the performance of the feature part of OTOD (the Equation (1)) decreases as  $\|\mu_i - \mu^{ood}\|_{TV}$  approaches to 0. In other words, Equation (1) can detect pronounced distribution shifts.

## IV. EXPERIMENTAL RESULTS

### A. Experimental Setup

**Datasets.** In our research, we utilize two common benchmarks to evaluate our methods: the CIFAR-10 [3] and CIFAR-100 [3] benchmarks. In the CIFAR-10 benchmark, the OOD datasets used for evaluation are CIFAR-100 [3], TIN [11], MNIST [12], SVHN [13], Texture [14], Places365 [15]. In the CIFAR-100 [3] benchmark, the OOD datasets used for

TABLE III

ABLATION OF THE INPUT OF OTOD ON THE CIFAR-100 BENCHMARK USING RESNET-18 AS THE BACKBONE AND THE TEMPERATURE  $T$  IS TAKEN AS 3. HERE WE REPORT THE MEAN VALUE OF FPR AND AUROC OVER 6 OOD DATASETS.

|       | Features | Logits | Probs | FPR@95↓      | AUROC ↑      |
|-------|----------|--------|-------|--------------|--------------|
| (i)   | ✓        | ✗      | ✗     | 62.98        | 74.54        |
| (ii)  | ✓        | ✓      | ✗     | 58.68        | 77.98        |
| (iii) | ✓        | ✓      | ✓     | <b>55.14</b> | <b>80.02</b> |

evaluation are CIFAR-100 [3], TIN [11], MNIST [12], SVHN [13], Texture [14], Places365 [15], respectively.

**Evaluation metrics.** We use the following metrics to evaluate the OOD detection performance: (i) the False Positive Rate (FPR) at 95% True Positive Rate; (ii) the Area Under the Receiver Operating Characteristic curve (AUROC); (iii) the in-distribution classification accuracy (ID ACC).

**Implementation details.** In the experiments, we use ResNet-18 [5] and WideResNet-28 [16] as backbones to perform OOD detection on the aforementioned datasets. To ensure fairness, all post-hoc methods use the same pre-trained model and are evaluated on one NVIDIA V100 GPU with Python 3.8.19, CUDA 11.3 + Pytorch 1.13.1. On the CIFAR-100 benchmark [3], the temperature of our method is set to  $T = 3$  for both ResNet-18 [5] and WideResNet-28 [16] architectures. On the CIFAR-10 benchmark [3], the temperature of our method is set to  $T = 10$  for both ResNet-18 [5] and WideResNet-28 [16] architectures. For both ResNet-18 [5] and WideResNet-28 [16] architectures,  $\alpha_1, \alpha_2, \alpha_3$  in equation (2) are all fixed to  $\frac{1}{3}$  on the CIFAR-10/100 [3] benchmarks. The resolution of the pre-trained model is  $32 \times 32$  and the training epoch is set to 100. The learning rate of the pre-trained model is taken as  $10^{-1}$  using SGD [17] as the optimizer. Our code is developed based on OpenOOD [18], [24].

**Baselines.** We compare OTOD with seven post-hoc OOD detection baselines, including MSP [2], ODIN [10], MDS [8], EBO [3], Gram [19], KLM [9], GEN [4]. We use OpenOOD [18], [24] to implement all the aforementioned methods. For ODIN [10], the temperature is set to  $T = 1000$  following the original work. For EBO [3], the temperature  $T$  is set to 1.

### B. OOD Detection Performance Results

**Evaluation on CIFAR-10.** The comparison results on the CIFAR-10 [6] benchmark are given in Table I. As shown in the first half of Table I, OTOD outperforms all the other scoring functions on various OOD datasets by a considerable margin using ResNet-18 as the backbone. Furthermore, it is noteworthy that OTOD surpasses GEN by 12.71% FPR@95 on Texture. From the second half of Table I, we can find that OTOD surpasses GEN by 12.51% on FPR@95 averaged on six OOD datasets taking WideResNet-28 as the backbone. These facts indicate that OTOD works for both ResNet-18 and WideResNet-28 architectures on the CIFAR-10 benchmark.

**Evaluation on CIFAR-100.** The results on CIFAR-100 benchmark is given in Table II. From the first half of Table

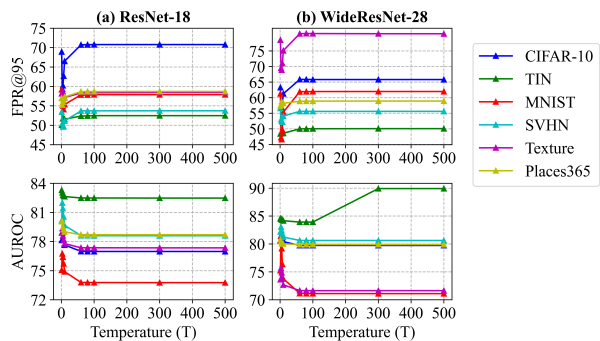


Fig. 3. (a)(b) Hyperparameter analysis on temperature  $T$  using ResNet-18 and WideResNet-28 as backbones on the CIFAR-100 benchmark.

II, we can find that OTOD achieves the best mean FPR@95 compared to other methods. Moreover, OTOD outperforms KLM by 18.19% FPR@95 and 3.67% AUROC on average. As shown in Table II, OTOD also achieves competitive results compared with GEN. In the second half of Table II, we can see that OTOD also works well using WideResNet-28 as the backbone.

### C. Ablation Analysis of OTOD Input

In this section, our purpose is to investigate the effects of each input in OTOD on the CIFAR-100 benchmark taking ResNet-18 as the backbone. By comparing setting (i), (ii), and (iii) in Table III, we can observe that the combination of features, logits and softmax probability inputs enhances the performance of OTOD scoring function. Note that, the AUROC of setting (i) is 5.48% lower than the AUROC of setting (iii).

### D. The Effect of Hyperparameters

In this section, we give a detailed analysis of the temperature  $T$  in OTOD on the CIFAR-100 benchmark taking ResNet-18 and WideResNet-28 as backbones. The results are shown in Fig. 3. From Fig. 3, we observe that when temperature  $T$  is small, increasing  $T$  can enhance the OOD detection performance on both ResNet-18 and WideResNet-28 architectures. While  $T$  is large, increasing  $T$  will harm the OOD detection results on both ResNet-18 and WideResNet-28 architectures.

## V. CONCLUSION

In this study, we introduce a novel scoring function, named OTOD, for detecting OOD samples. We calculate OOD scores for test samples using Wasserstein-1 distances, which do not require the use of any in-distribution data during the OOD testing phase. Afterward, We leverage information from feature, logits, and softmax probability spaces to achieve better OOD detection performance using our optimal transport-based score function. Moreover, we apply the temperature scaling technique to further improve the detection result. Both theoretical and experimental results demonstrate the superior performance of our score function.

## REFERENCES

- [1] Nguyen, Anh, Jason Yosinski, and Jeff Clune. "Deep neural networks are easily fooled: High confidence predictions for unrecognizable images." In *2015 IEEE Conference on Computer Vision and Pattern Recognition*, pp. 427-436. IEEE Computer Society, 2015.
- [2] Hendrycks, Dan, and Kevin Gimpel. "A Baseline for Detecting Misclassified and Out-of-Distribution Examples in Neural Networks." In *International Conference on Learning Representations*. 2017.
- [3] Liu, Weitang, Xiaoyun Wang, John D. Owens, and Yixuan Li. "Energy-based out-of-distribution detection." In *Proceedings of the 34th International Conference on Neural Information Processing Systems*, pp. 21464-21475. 2020.
- [4] Liu, Xixi, Yaroslava Lochman, and Christopher Zach. "Gen: Pushing the limits of softmax-based out-of-distribution detection." In *Proceedings of the IEEE/CVF Conference on Computer Vision and Pattern Recognition*, pp. 23946-23955. 2023.
- [5] He, Kaiming, Xiangyu Zhang, Shaoqing Ren, and Jian Sun. "Deep residual learning for image recognition." In *Proceedings of the IEEE Conference on Computer Vision and Pattern Recognition*, pp. 770-778. 2016.
- [6] Krizhevsky, Alex. "Learning Multiple Layers of Features from Tiny Images." (2009). Citeseer.
- [7] Villani, Cédric. *Optimal transport: old and new*. Vol. 338. Berlin: springer, 2009.
- [8] Lee, Kimin, Kibok Lee, Honglak Lee, and Jinwoo Shin. "A simple unified framework for detecting out-of-distribution samples and adversarial attacks." In *Proceedings of the 32nd International Conference on Neural Information Processing Systems*, pp. 7167-7177. 2018.
- [9] Hendrycks, Dan, Steven Basart, Mantas Mazeika, Andy Zou, Joseph Kwon, Mohammadreza Mostajabi, Jacob Steinhardt, and Dawn Song. "Scaling Out-of-Distribution Detection for Real-World Settings." In *International Conference on Machine Learning*, pp. 8759-8773. PMLR, 2022.
- [10] Liang, Shiyu, Yixuan Li, and R. Srikant. "Enhancing The Reliability of Out-of-distribution Image Detection in Neural Networks." In *International Conference on Learning Representations*. 2018.
- [11] Le, Ya, and Xuan Yang. "Tiny imagenet visual recognition challenge." *CS 231N 7*, no. 7 (2015): 3.
- [12] Deng, Li. "The mnist database of handwritten digit images for machine learning research [best of the web]." *IEEE signal processing magazine* 29, no. 6 (2012): 141-142.
- [13] Netzer, Yuval, Tao Wang, Adam Coates, Alessandro Bissacco, Baolin Wu, and Andrew Y. Ng. "Reading digits in natural images with unsupervised feature learning." In *NIPS workshop on deep learning and unsupervised feature learning*, vol. 2011, no. 2, p. 4. 2011.
- [14] Cimpoi, Mircea, Subhransu Maji, Iasonas Kokkinos, Sammy Mohamed, and Andrea Vedaldi. "Describing textures in the wild." In *Proceedings of the IEEE Conference on Computer Vision and Pattern Recognition*, pp. 3606-3613. 2014.
- [15] Zhou, Bolei, Agata Lapedriza, Aditya Khosla, Aude Oliva, and Antonio Torralba. "Places: A 10 million image database for scene recognition." *IEEE transactions on pattern analysis and machine intelligence* 40, no. 6 (2017): 1452-1464.
- [16] Zagoruyko, Sergey, and Nikos Komodakis. "Wide Residual Networks." In *British Machine Vision Conference 2016*. British Machine Vision Association, 2016.
- [17] Robbins, Herbert, and Sutton Monro. "A stochastic approximation method." *The annals of mathematical statistics* (1951): 400-407.
- [18] Zhang, Jingyang, Jing Kang Yang, Pengyun Wang, Haoqi Wang, Yueqian Lin, Haoran Zhang, Yiyu Sun et al. "OpenOOD v1.5: Enhanced Benchmark for Out-of-Distribution Detection." In *NeurIPS 2023 Workshop on Distribution Shifts: New Frontiers with Foundation Models*.
- [19] Sastry, Chandramouli Shama, and Sageev Oore. "Detecting out-of-distribution examples with gram matrices." In *International Conference on Machine Learning*, pp. 8491-8501. PMLR, 2020.
- [20] Morteza, Peyman, and Yixuan Li. "Provable guarantees for understanding out-of-distribution detection." In *Proceedings of the AAAI Conference on Artificial Intelligence*, vol. 36, no. 7, pp. 7831-7840. 2022.
- [21] Gretton, Arthur, Karsten M. Borgwardt, Malte J. Rasch, Bernhard Schölkopf, and Alexander Smola. "A kernel two-sample test." *The Journal of Machine Learning Research* 13, no. 1 (2012): 723-773.
- [22] McInnes, Leland, John Healy, Nathaniel Saul, and Lukas Großberger. "UMAP: Uniform Manifold Approximation and Projection." *Journal of Open Source Software* 3, no. 29 (2018): 861.
- [23] Janati, Hicham. "Advances in Optimal transport and applications to neuroscience." PhD diss., Institut Polytechnique de Paris, 2021.
- [24] Yang, Jing Kang, Pengyun Wang, Dejian Zou, Zitang Zhou, Kunyuan Ding, WENXUAN PENG, Haoqi Wang et al. "OpenOOD: Benchmarking Generalized Out-of-Distribution Detection." In *Thirty-sixth Conference on Neural Information Processing Systems Datasets and Benchmarks Track*.